JOURNAL OF GEOPHYSICAL RESEARCH, VOL. 105, NO. E6, PAGES 15,051–15,059, JUNE 25, 2000

Thermal infrared spectroscopy of Europa and Callisto

Franklin P. Mills[1] and Michael E. Brown

Geological and Planetary Sciences, California Institute of Technology, Pasadena, California

Abstract. The trailing hemispheres of Europa and Callisto were observed at $9-13$ μm, and a spectrum of Europa with better spectral resolution and a better signal-to-noise ratio than was previously possible has been derived. The ratio spectrum of the two satellites has a signal-to-noise ratio of approximately 30 for a spectral resolving power of approximately 50. The disk-integrated, effective color temperature ratio for the two satellites is consistent with broadband, thermal infrared photometry from previous ground-based studies and from the Galileo photopolarimeter radiometer. The ratio spectrum was combined with the average Voyager 1 spectrum of Callisto to obtain a $9-13$ μm spectrum of Europa with a signal-to-noise ratio that is a factor of 10 better than that in the average Voyager spectrum of Europa. After convolving the measured spectrum to the expected width of water ice emissivity features, ~ 1 μm, no spectral features that could be attributed to water ice on the surface of Europa are apparent at the $0.6-0.7\%$ level. The absence of spectral features attributable to water ice is consistent with the proposal that the equatorial region of Europa that was observed may be composed primarily of a heavily hydrated mineral. The absence of water ice features may also be the result of a large fractional abundance of fine particles, such as that found on the surface of the Moon.

1. Introduction

Most ground-based observations of the icy Galilean satellites have focused on the visual and short wave infrared ($1-3$ μm) regions where ices and clay minerals have absorption features that can be diagnostic of composition (see reviews by *Johnson and Pilcher* [1977], *Clark et al.* [1986], and *Calvin et al.* [1995]). The Near-Infrared Mapping Spectrometer (NIMS) on Galileo has extended this coverage to 5 μm [*Carlson et al.*, 1996] and the photopolarimeter radiometer on Galileo has collected imagery at 37 μm, but no data will be collected by Galileo at intermediate wavelengths. Consequently, no spectra have been published for the thermal infrared region, TIR ($7-14$ μm), since Voyager 1 and 2 [*Hanel et al.*, 1979; *Spencer*, 1987a], even though these wavelengths have been useful in Earth remote sensing studies for discriminating surface composition [*Kahle and Goetz*, 1983] and soil characteristics [*Salisbury and D'Aria*, 1992]. There have been significant advances in instrumentation since the Voyager infrared imaging spectrometer, so new spectra of Europa and Callisto were obtained to determine if better thermal infrared spectra could help constrain the surface characteristics of these satellites.

Observational, laboratory, and modeling studies over the past two decades led to the development of several models for the surface properties of Europa and Callisto. Although none of the published models explains all of the observed spectral features, several give reasonable fits to the observed $0.4-3$ μm spectra for Callisto [*Clark et al.*, 1986; *Spencer*, 1987b; *Roush et al.*, 1990; *Calvin and Clark*, 1991, 1993; *Calvin et al.*, 1995]. The primary differences among the proposed Callisto surface models are the grain size, the degree of segregation of the ice and nonice components, and the relative abundance of water ice. The identity of the nonwater ice component(s) of Callisto's surface was poorly constrained by pre-Galileo observations, but recent data have identified spectral features consistent with hydrated minerals and CO_2 [*Carlson et al.*, 1996], organics and compounds containing SH [*McCord et al.*, 1997], and SO_2 [*Lane and Domingue*, 1997; *McCord et al.*, 1997; *Noll et al.*, 1997].

Prior to Galileo the standard model for Europa's surface [*Calvin and Clark*, 1991] was medium to large particles (of order hundreds of micrometers to centimeters in size) with $\gtrsim 95$ wt % ice (as revised by *Calvin*

[1]Now at Jet Propulsion Laboratory, California Institute of Technology, Pasadena, California

Paper number 1999JE001163.
0148-0227/00/1999JE001163$09.00

et al. [1995]). More recently, *Belton et al.* [1996] found evidence that the surface of Europa was heterogeneous when they located two regions for which the near-infrared reflectances differed but the visual albedos were approximately the same. They attributed the near-infrared differences to different grain sizes in the two regions. *Carlson et al.* [1996], in the same issue, reported that laboratory spectra of a fine-grained frost overlying ice (as originally proposed by *Clark* [1981]) gave the best match to the NIMS spectra of Europa's north pole. *Domingue and Verbiscer* [1997] then reexamined the visual photometry data for Europa and concluded that if Europa's surface has a grain size distribution similar to that for the Moon, then the surface must be fairly transparent and must have a porosity that is 1.5 times larger than that for the Moon. Alternatively, *McCord et al.* [1998] reported the detection of a hydrated mineral component on the surface of Europa and proposed the hydrated mineral was a mixture of heavily hydrated carbonates and sulfates. From their analysis a large fraction of the equatorial region imaged by NIMS was composed primarily of the hydrated mineral, although the north polar region of Europa appeared to be nearly pure water ice.

Thermal infrared observations have the potential to contribute additional information on the characteristics of the surfaces of Callisto and Europa. TIR spectra of a body with little or no atmosphere are determined by four primary variables: the composition of the surface particles, the size of the particles, the relative abundance of each component, and the manner in which particles of differing composition (or differing physical temperatures) are interspersed. Near surface temperature gradients also can affect remotely observed thermal infrared spectra, but *Henderson and Jakosky* [1994] showed that the spectral contrast in the Reststrahlen bands increases as a result of the thermal gradient present on a body with no atmosphere when the surface is heated from below as has been proposed for the heating due to solar insolation on the icy Galilean satellites [*Urquhart and Jakosky,* 1996].

Both water ice and silicates have emissivity features in the thermal infrared that are potentially diagnostic of composition when the materials are in medium-to-large particles (radii larger than or of order hundreds of micrometers) with only minimal amounts of small particles (radii less than or of order 50 micrometers): water ice in the $11 - 13$ μm region [*Warren,* 1984; *Spencer,* 1987a; *Salisbury et al.,* 1994] and silicates in the $7.5 - 9.5$ μm region [e.g., *Nash et al.,* 1993, and references therein].

Two spectral features within the TIR that are potentially diagnostic of composition are the location of the Reststrahlen bands and the location of the Christiansen feature. Reststrahlen bands are the fundamental stretching vibration bands for adjacent atoms in a solid lattice, such as for Si-O. These vibration bands are sufficiently intense that "first surface reflection" or "surface scattering" occurs for a smooth solid surface. This leads to a minimum at these wavelengths in an emission spectrum. For a highly ordered silicate, such as quartz, the spectral contrast can be as large as 40% [*Salisbury and D'Aria,* 1992] for a freshly cut, smooth surface near 9.3 μm. As the particle size in a silicate powder decreases, the spectral contrast in the Reststrahlen bands also decreases [e.g., *Salisbury and Wald,* 1992]. For larger particles, this is due to the multiple reflections that can occur among the particles, but for powders with optically thin particles separated by more than one wavelength, the particles act as independent, incoherent scatterers for which "volume scattering" dominates over "surface scattering" [*Salisbury,* 1993]. Typical ground laboratory samples and lunar regolith samples have a sufficient number of small particles (smaller than 10 micrometers) so that the spectral contrast in the Reststrahlen bands is greatly reduced [*Salisbury et al.,* 1997; *Moersch and Christensen,* 1995]. "Volume scattering" generally dominates when the absorption coefficient of the material is sufficiently weak so that photons can pass through individual particles during the scattering process. The spectral contrast in regions that are dominated by "volume scattering" can either increase or decrease with decreasing particle size (and the accompanying increase in the number of scattering surfaces), depending on whether the center of the absorption band is optically thick or thin (respectively) [*Salisbury,* 1993]. For fine-grained silicates, the Christiansen feature is often easier to determine than the location of the Reststrahlen band [*Nash et al.,* 1993], but the principal Christiansen feature for many silicates lies near the short-wavelength edge of the $8-14$ μm window through the terrestrial atmosphere. The Christiansen feature occurs where the real part of the refractive index is equal, or close, to that of the surrounding medium and the imaginary part of the refractive index is sufficiently small so that absorption is minimum. This leads to a local maximum in an emission spectrum. Comparable systematic studies for water ice spectral features in the $8 - 14$ μm region have not been published.

The maximum measured spectral contrast in the Reststrahlen band for water ice near 12.3 μm is 6% for a smooth distilled water ice surface (i.e., a Fresnel surface) [*Salisbury et al.,* 1994]. This is much smaller than in the 9.3 μm silicate Reststrahlen band. Unlike the situation for the silicate Reststrahlen bands, the change of spectral contrast with particle size for water ice has not been clearly determined. Calculations using a collection of spheres as a model for frost and snow by *Dozier and Warren* [1982] suggest the spectral contrast at $8 - 15$ μm is insensitive to spherical particle size over the range of $50 - 1000$ micrometers. Laboratory measurements of natural terrestrial snow and frost that included partially melted and refrozen surfaces and irregularly shaped water ice grains by *Salisbury et al.* [1994], however, found the spectral contrast in the water ice Reststrahlen band increased with increasing particle size. This trend in the

measured results could be due to increased Fresnel reflections from flat, welded surfaces in the snow samples, if these sources were not considered in deriving the "typical" particle size of the samples (G. Hansen, personal communication, 2000). *Rinsland et al.* [1998] have also noted differences between extinction measurements for small terrestrial cirrus ice particles and calculated extinctions based on laboratory measurements of optical constants.

The qualitative differences between the collection of spheres model predictions and the existing measurements of natural terrestrial snow suggest there are problems with the model calculations, the characterization of the laboratory samples, the laboratory measurements, or all three. For interpretation of our observations we have relied on the measurements of water ice emissivity by *Salisbury et al.* [1994] in which spectral contrast for water ice in the thermal infrared increases as the particle size increases. Further laboratory measurements in the $8 - 14$ μm region and comparisons to numerical calculations are needed.

Quantitative estimates of the relative abundances of surface materials from remote sensing data depends critically on the manner in which the components are interspersed (mixed) and the relative physical temperatures of the components. *Thomson and Salisbury* [1993] showed that spectra of intimate mixtures of silicate particles of differing compositions in the 75-250 micrometer size range behave as linear mixtures (by volume) of the component materials. However, an intimate mixture of water ice with other material would have nonlinear effects due to the relatively large differences between the imaginary indices of refraction of the component materials [*Clark and Lucey,* 1984]. If, on the other hand, there is large-scale (macroscopic) separation of the components and the components are at different physical temperatures, then the signature of the component that has the higher temperature will be enhanced relative to the signature of the cooler component, assuming both components have the same emissivity [e.g., *Spencer,* 1987c].

Ground-based TIR observations of the icy Galilean satellites in the 1970s measured only broadband brightness temperatures (reviewed by *Morrison* [1977]). Since then, no ground-based thermal emission spectra have been published, although thermal infrared spectra were obtained by Voyager 1 and 2. *Hanel et al.* [1979] found "contrast differences on the order of 1 percent or less" in Voyager 1 spectra of Europa and Callisto. *Spencer* [1987a] also concluded there were no unambiguous spectral features in the Voyager spectra of Europa and Callisto. However, the Voyager spectra were relatively noisy for wavelengths $\lesssim$ 13 μm for Europa and for wavelengths $\lesssim$ 8 μm for Callisto, so Voyager probably would not have been able to detect features due to water ice on Europa nor features due to silicates on Callisto.

2. Observations and Processing

Callisto and Europa were observed on July 1, 1996, from 0630 to 1130 UT from Palomar Observatory using the 5 m Hale Telescope and SpectroCam-10 [*Hayward et al.*, 1993]. SpectroCam-10 was used in its low-resolution spectrographic mode (128 spectral $\times$ 64 spatial pixels) with spectral resolving power $\sim$ 50 for a $2'' \times 16''$ slit and a pixel scale of $0.25''$. Spectra were collected at three grating positions to provide complete coverage of the $8 - 14$ μm region.

Data were acquired using a sequence of 4.75 Hz, $8''$ chops and $8''$ nods arranged to permit proper removal of background radiance from the measured thermal emission from the satellites. The on-source integration time for individual object and sky spectra was 30 s; Callisto and Europa were observed, alternately, for intervals of 15 min each.

Figure 1a shows the measured spectra of Callisto and Europa from 51 and 45 min of on-source integration, respectively. Figure 1b shows the ratio of the averaged spectra for the two satellites (Callisto/Europa).

The solar phase angle was approximately 0.7°. The trailing hemisphere of Callisto was observed at orbital longitudes $280° - 290°$, and the trailing hemisphere of Europa was observed at orbital longitudes $210° - 230°$. Zenith angles ranged from $56° - 68°$ and typical seeing was $1''$.

Observing conditions were nonphotometric; Palomar had been closed the preceding 36 hours due to ash from forest fires, and residual smoke from those fires was present at the time of our observations. Thermal emission from the smoke should have been removed by the nodding and chopping sequence. Assuming the smoke concentration varied slowly with time, the effects of scattering by the smoke particles should not be present in the ratio spectrum we derive because scattering by the smoke would have the same effect on both the Europa and the Callisto spectra. The visual optical depth of the smoke was small, based on daytime observations the evening before the thermal emission measurements.

3. Results

The ratio spectrum (Figure 1b) can be used directly to constrain the ratio between the disk-integrated, effective, color temperatures of Callisto and Europa (Figure 2). The locus of best fit temperature ratios indicated by the solid line in Figure 3 are statistically equivalent to the fit in Figure 2. The present color temperature ratio is consistent with previous ground-based brightness temperatures for the $8 - 12$ μm wavelength region, as shown in Figure 3. As discussed by *Morrison* [1977], the two brightness temperature ratios that lie furthest from the present result are from *Gillett et al.* [1970] and may be biased due to incorrect satellite diameters and/or incorrect calibration procedures. The present color temperature ratio is also consistent with

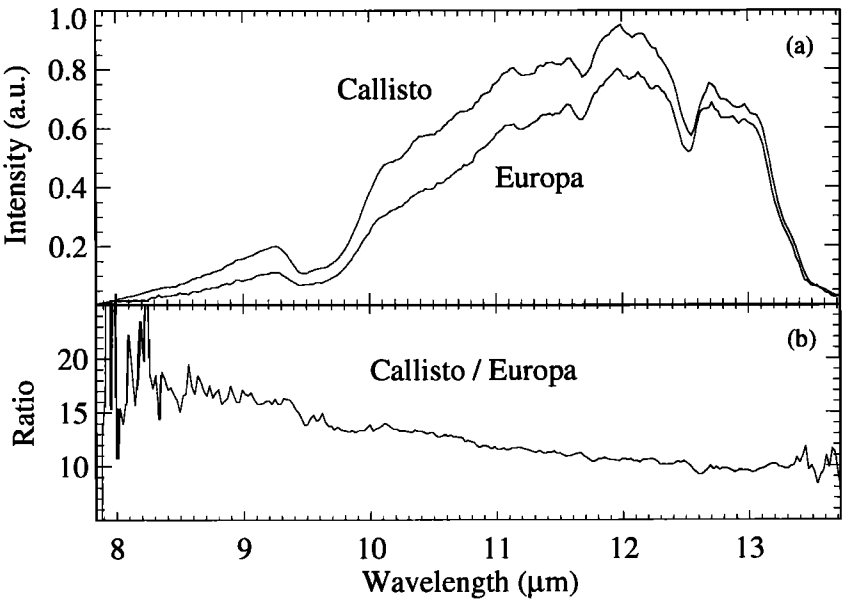

Figure 1. (a) Disk-integrated thermal emission spectra of the trailing hemispheres of Callisto and Europa measured with SpectroCam-10 at Palomar Observatory, July 1, 1996. The prominent absorption features in these spectra are due to absorption in the terrestrial atmosphere, primarily by O_3 and CO_2. (b) Ratio of spectra from Figure 1a.

the brightness temperatures measured near the subsolar point on Europa by the Galileo photopolarimeter radiometer [*Spencer et al.,* 1999].

To look for the presence of spectral features that might be produced by water ice on the surface of Europa, we combined our ratio spectrum, Figure 1b, with the average spectrum of Callisto collected by Voyager 1 [*Spencer,* 1987a] to synthesize a spectrum of Europa, Figure 4a. The average Voyager 1 spectrum of Callisto from Figure 4 of *Spencer* [1987a] was digitized, converted from brightness temperatures to radiances, divided by our ratio spectrum (Figure 1b), and then converted from radiances into brightness temperatures. This effectively gives [Voyager Callisto]/[{Palomar Callisto}/{Palomar Europa}]. The long-dashed curve in Figure 4a was digitized from the average Voyager 2 spectrum of Europa in Spencer's Figure 4.

None of the spectral features in our derived Europa spectrum at $10 - 13$ μm are significant. All lie at the wings of telluric absorption bands, so they are likely due to incomplete cancellation of the telluric bands in the ratio spectrum. Further, laboratory measurements [*Salisbury et al.,* 1994] and numerical calculations [*Dozier and Warren,* 1982] indicate that absorption features due to water ice would be $\sim 1 - 1.5$ μm peak to trough. The dominant spectral features in Figures 2 and 4a have much narrower widths, so they are not due to water ice on the surface of Europa. The absence of significant features in the present spectra is consistent with previous findings [*Hanel et al.,* 1979; *Spencer,* 1987a].

The dominant source of "noise" in our spectrum is the incomplete cancellation of telluric absorption features. If the measured ratio spectrum is smoothed using a triangular kernel function with full width at half maximum (FWHM) of 0.2 μm, Figure 2, then the RMS deviation from the blackbody ratio is $< 1.5\%$ in the region where water ice features would be expected. Convolving our Europa spectrum to the expected $1 - 1.5$ μm FWHM gives an upper limit of $\sim 0.6 - 0.7\%$ for possible water ice absorption features in our Europa spectrum. This noise level is at least a factor of 10 smaller than in any previously published spectrum for < 13 μm for Europa. Our signal level is sufficiently poor at wavelengths less than 9 μm and greater than 13 μm that features outside this range also should not be considered significant.

4. Discussion

Numerical modeling would be required to quantitatively interpret our nondetection, but the best existing numerical calculations do not qualitatively agree with the best existing laboratory measurements of natural terrestrial snows (section 1). Consequently, it is not possible to provide a definitive numerical interpretation of our nondetection. It is important to note, though, that our nondetection at the $\sim 0.6 - 0.7\%$ level is significant at the 1 standard deviation level even using the existing numerical calculations. Our observation suggests that if water ice is present on Europa's surface, then it produces a spectral contrast that is below our sensitivity. Alternatively, water ice is not the primary constituent of the region on Europa's surface that produces the thermal emission we have observed.

Laboratory measurements of terrestrial snow find that

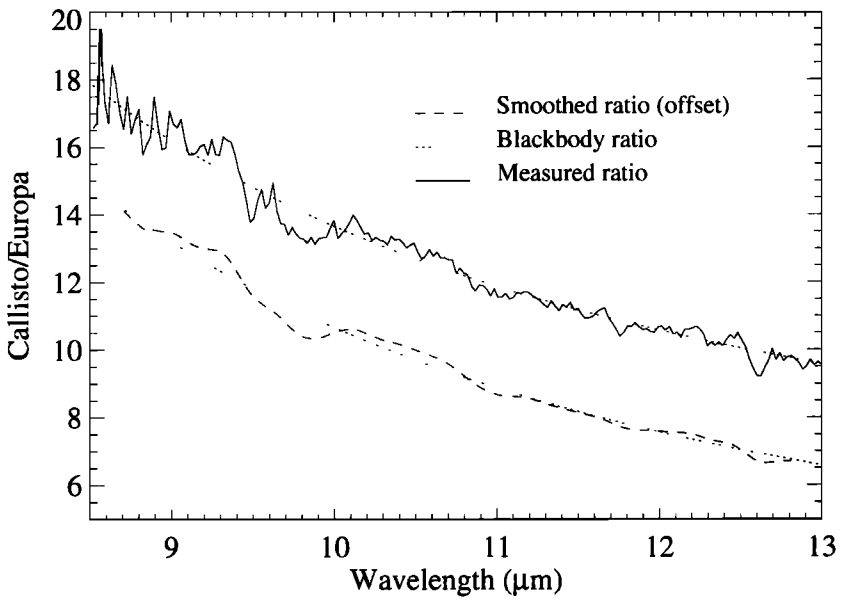

Figure 2. The solid curve is the measured ratio spectrum from Figure 1b. The dashed curve is the measured ratio spectrum convolved with a triangular kernel function with FWHM of 0.2 μm, offset by a fixed amount for clarity of presentation. The dotted curve is the ratio of a 151 K and a 130 K blackbody that has been scaled to account for such factors as the differences in projected area and observing time for the two satellites. This scaling also accounts for any differences in flux produced by temporal variations in the observing conditions. The RMS deviation of the measured ratio spectrum from the blackbody ratio is 3% for the $8.5 - 13$ μm region and 2% for the $10 - 13$ μm region. The RMS deviation of the smoothed measured ratio spectrum from the blackbody ratio is 2% for the $8.5 - 13$ μm region and $< 1.5\%$ for the $10 - 13$ μm region.

spectral contrast is reduced by either an intimate mixture of water ice with another material or the presence of abundant small size ice particles. We are not aware of any mixing study that has been done for water ice and minerals in the thermal infrared region, so there are uncertainties in the spectral contrasts that should be expected from such a mixture. If we make the assumption, probably incorrect, that the spectral mixing is linear, then our upper limit of $\sim 0.6 - 0.7\%$ on possible water ice spectral features, when combined with the *Salisbury et al.* [1994] laboratory measurements, implies that the surface region of Europa we observed contains less than 40% water ice, if the particles are $\gtrsim$ 500 micrometer in radius. The measured spectral contrast in laboratory water ice frosts and fine-grained terrestrial snow is sufficiently small that our observation places no constraint on the presence or absence of these fine-grained materials on the surface of Europa. Our observations can be reconciled with the proposal by *Calvin and Clark* [1991] (as revised by *Calvin et al.* [1995]) that Europa's surface is composed of $\gtrsim$ 95 wt % water ice in particles that are of order hundreds of micrometers to centimeters in size only if the nonwater ice material were strongly absorbing but spectrally neutral in the $10 - 13$ μm region or the spectral mixing were highly nonlinear.

As a different assessment of our sensitivity to water ice, we compared our derived Europa spectrum (Figure 4b) to the measured laboratory spectra for terrestrial snow and frost from *Salisbury et al.* [1994] by computing the cross correlations between these spectra. As a control on this analysis, we also computed cross correlations between the laboratory spectra with and without Gaussian noise. The cross correlations among the laboratory snow spectra indicate a clear signal for the presence of snow should be present even if 1.5% Gaussian noise is added to the laboratory spectrum. No such correlation was found between the derived Europa spectrum and the laboratory snow spectra from *Salisbury et al.* [1994]. From our cross correlation analysis we found it would not be possible to detect fine-grained water ice frost if the noise level was 1.5%.

One argument against small particle sizes for water ice on Europa is that fine ice grains will grow relatively rapidly into larger particles [*Clark et al.*, 1986] as a result of the constant migration of water molecules in the vapor phase and the preferential loss of smaller ice grains via sputtering. *Carlson et al.* [1996] found evidence that this process may have occurred on the surface of Ganymede, although there are uncertainties in their interpretation and the surface temperatures on Ganymede are significantly warmer than those on Europa. However, the grain size distribution assumed by *Domingue and Verbiscer* [1997] contains a large fractional abundance of small particles and they find a reasonable match to the visual photometry observations for

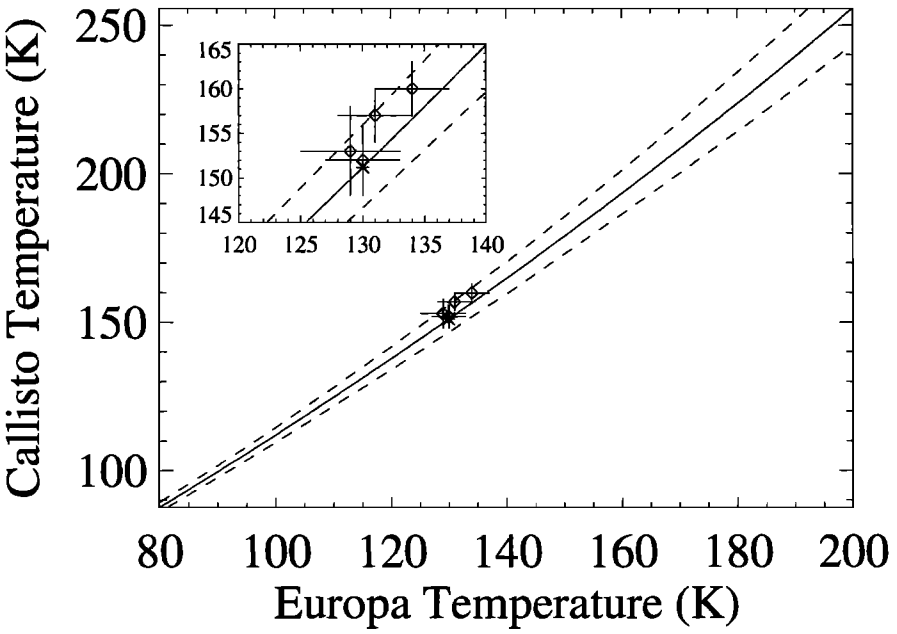

Figure 3. The solid line is the effective temperature for Callisto that gives the best fit to the measured ratio spectrum as a function of the effective temperature for Europa. The diamonds (with error bars) are the broadband brightness temperatures from the ground-based thermal infrared photometry reviewed by *Morrison* [1977]. The color temperature ratio used in Figure 2 is marked with an asterisk. All points along the solid line are statistically equivalent in terms of the quality of the fit to the measured ratio spectrum. The dashed lines are the estimated uncertainty in the effective color temperature ratio. They have an RMS deviation from the measured ratio spectrum that is equivalent to that for the blackbody temperature pairs 147 and 130 K and 155 and 130 K.

Europa by assuming the porosity of Europa's surface is 1.5 times that for the Moon.

Another interpretation for the lack of water ice features in the thermal infrared spectrum of Europa is that water ice is not present on the portion of Europa's surface that we observed. Our spectra are most sensitive to the regions within the field of view with highest emissivity and/or highest temperature, such as near the subsolar point. *McCord et al.* [1999] have proposed that the subsolar region for our observations ($210° - 230°$ orbital longitude) is primarily ($60-80\%$) nonwater ice material. They proposed that this region is dominated by highly hydrated minerals which might explain the absence of water ice features in our Europa spectrum. Laboratory and field measurements of pure samples of terrestrial hydrated salts in the $9.5 - 12.5$ μm region find that many of these salts are featureless at the $\sim 1\%$ level in this wavelength region [*Crowley and Hook,* 1996]. Pure borate salts have several broad $\sim 10\%$ peak-to-peak features in the $9.5 - 12.5$ μm region that are not found in our Europa spectrum. Pure carbonate salts have a 0.2 μm wide feature of $\sim 10\%$ depth near 11.7 μm that might be present in our high-resolution ratio spectrum Figure 2, but no significant feature is present for the noise level of our observation at that spectral resolution. Sulfate salts are likely to be found on Europa based on the detections of SO_2 on Europa, but the sulfate group spectral features are at $8.5 - 9.2$ μm where the noise level in our Europa spectrum is relatively poor.

5. Conclusions

The trailing hemispheres of Europa and Callisto were observed, and a $10 - 13$ μm spectrum of Europa with better spectral resolution (resolving power of about 50) and a factor of 10 better signal-to-noise ratio than was previously possible has been derived. The disk-integrated, effective color temperature ratio for the two satellites is consistent with broadband, thermal infrared photometry.

Consistent with previous studies [*Hanel et al.,* 1979; *Spencer,* 1987a], no spectral features that can be definitely attributed to water ice on the surface of Europa were found at the $\gtrsim 1\%$ level. Comparison to existing laboratory spectra of terrestrial ice, snow, and frost [*Salisbury et al.,* 1994] indicates that the nondetection is significant. However, further laboratory and numerical modeling studies are needed to quantify the significance of the apparent nondetection of water ice features in the Europa spectrum and to reconcile the apparent qualitative, as well as quantitative, discrepancies between numerical models and laboratory measurements [*Dozier and Warren,* 1982; *Salisbury et al.,* 1994; *Wald,* 1994].

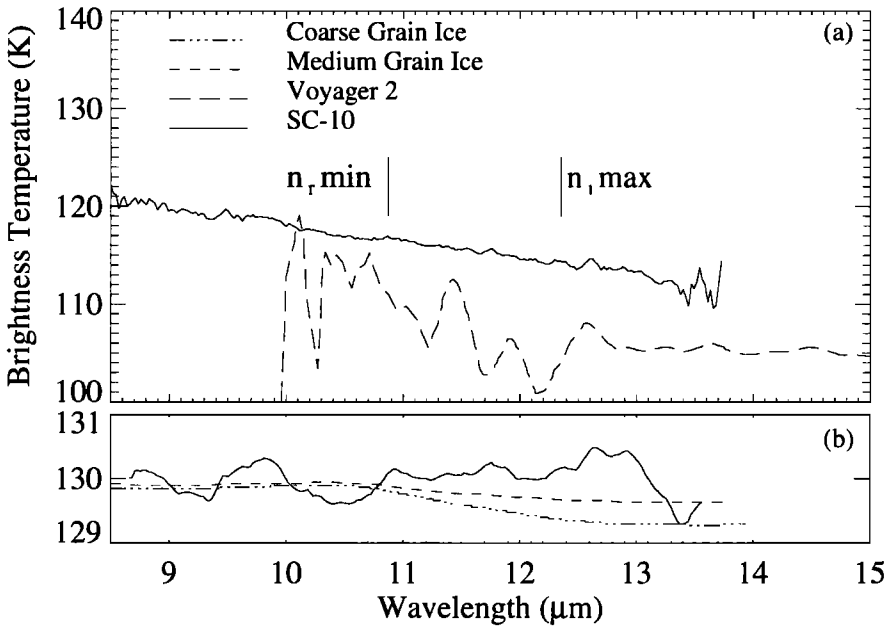

Figure 4. (a) The long-dashed curve is the average Voyager 2 spectrum of Europa from *Spencer* [1987a]. It is an average of all spectra with 22-μm brightness temperature warmer than 90 K, a total of 53 spectra. The spectrum was smoothed by Spencer with a boxcar filter of width 14 cm^{-1}. The labels n_i max and n_r min mark the locations where water ice features would be expected [*Warren,* 1984; *Spencer,* 1987a]. The solid curve is the Europa spectrum derived from combining the ratio spectrum in Figure 1b with the average Voyager 1 spectrum of Callisto from Spencer as discussed in section 3. No features are found above our noise level at the locations where they would be expected for water ice. (The temperature offset between our derived spectrum and that obtained by Voyager 2 for Europa arises in part because we used Voyager 1 spectra from the relatively warm afternoon quadrant of Callisto to scale our ratio spectrum, whereas the Voyager 2 spectra of Europa were collected near Europa's evening terminator.) (b) The solid curve was derived by first combining the *smoothed* ratio spectrum in Figure 2 with the average Voyager 1 spectrum of Callisto from Spencer. The linear trend of decreasing brightness temperature with increasing wavelength in Figure 4a was then removed by a linear least squares fit. The other two curves are calculated spectra for medium- and coarse-grained snow using an assumed physical temperature of 130 K and using Kirchoff's law to convert the reflectance data from Figure 3 of *Salisbury et al.* [1994] to emissivities.

The apparent absence of water ice features in the $10-13$ μm spectrum of Europa probably is consistent with the result obtained by *McCord et al.* [1998], but laboratory measurements are necessary to confirm this. They found that the equatorial region of Europa may be composed primarily of a heavily hydrated mineral, rather than water ice. The apparent absence of water ice features in the $10-13$ μm spectrum of Europa may also just be the result of a large fractional abundance of fine particles, such as that assumed by *Domingue and Verbiscer* [1997] in their modeling of visual photometry observations. Our observations can be reconciled with the model proposed by *Calvin and Clark* [1991] (as revised by *Calvin et al.* [1995]) only if the nonwater ice material were strongly absorbing but spectrally neutral in the $0.5-13$ μm region or if the spectral mixing were highly nonlinear. Modeling of the full $1-13$ μm region is required to examine what nonwater ice material could satisfy the existing observations.

Our ratio spectrum, Figure 1b, is too noisy at < 8.5 μm to place a significant constraint on possible silicate Reststrahlen bands in Callisto's spectrum. As has also been noted in previous studies [*Hanel et al.,* 1979; *Spencer,* 1987a], however, there are no definite spectral features at the 1% level in the Voyager 1 spectrum of Callisto at $8-14$ μm. The absence of silicate features in the Voyager 1 Callisto spectrum suggests either they were not present in the observed regions or the presence of a large fractional abundance of fine particles, such as that found on the surface of the Moon.

Future thermal infrared emission studies of the icy Galilean satellites will likely need to locate the wavelengths of the Christiansen features of the surface materials if they want to determine the composition of the surface materials. Signal-to-noise ratios of ~ 1000 are likely to be needed for these observations.

Acknowledgments. The observations described in this paper would not have been possible without the assistance of the Palomar Observatory staff and Tom Hayward. Helpful reviews of the manuscript were provided by Eric Gai-

dos, Gary Hansen, Jack Salisbury, John Spencer, and Albert Yen. Michael E. Brown is an Alfred P. Sloan Research Fellow. This is contribution 5766 from the Division of Geological and Planetary Sciences of the California Institute of Technology.

References

Belton, M.J.S., et al., Galileo's first images of Jupiter and the Galilean satellites, *Science*, *274*, 377-385, 1996.

Buratti, B.J., Photometry and surface structure of the icy Galilean satellites, *J. Geophys. Res.*, *100*, 19,061-19,066, 1995.

Calvin, W.M., and R.N. Clark, Modeling the reflectance spectrum of Callisto 0.25 to 4.1 μm, *Icarus*, *89*, 305-317, 1991.

Calvin, W.M., and R.N. Clark, Spectral distinctions between the leading and trailing hemispheres of Callisto: New observations *Icarus*, *104*, 69-78, 1993.

Calvin, W.M., R.N. Clark, R.H. Brown, and J.R. Spencer, Spectra of the icy Galilean satellites from 0.2 to 5 μm: A compilation, new observations, and a recent summary, *J. Geophys. Res.*, *100*, 19,041-19,048, 1995.

Carlson, R., et al., Near-infrared spectroscopy and spectral mapping of Jupiter and the Galilean satellites: Results from Galileo's initial orbit, *Science*, *274*, 385-388, 1996.

Clark, R.N., Water frost and ice: The near-infrared spectral reflectance 0.65 – 2.5 μm, *J. Geophys. Res.*, *86*, 3087-3096, 1981.

Clark, R.N., and P.G. Lucey, Spectral properties of ice-particulate mixtures and implications for remote sensing, *J. Geophys. Res.*, *89*, 6341-6348, 1984.

Clark, R.N., F.P. Fanale, and M.J. Gaffey, Surface composition of satellites, in *Satellites*, edited by J.A. Burns and M.S. Matthews, pp. 463-472, Univ. of Ariz. Press, Tucson, 1986.

Crowley, J.K., and S.J. Hook, Mapping playa evaporite minerals and associated sediments in Death Valley, California, with multispectral thermal infrared images, *J. Geophys. Res.*, *101*, 643-660, 1996.

Domingue, D., and A. Verbiscer, Re-analysis of the solar phase curves of the icy Galilean satellites, *Icarus*, *128*, 49-74, 1997.

Dozier, J., and S.G. Warren, Effect of viewing angle on the infrared brightness temperature of snow, *Water Resour. Res.*, *18*, 1424-1434, 1982.

Gillett, F.C., K.M. Merrill, and W.A. Stein, Albedo and thermal emission of Jovian satellites I - IV, *Astrophys. Lett.*, *6*, 247-249, 1970.

Hanel, R., B. Conrath, M. Flasar, V. Kunde, P. Lowman, W. Maguire, J. Pearl, J. Pirraglia, and R. Samuelson, Infrared observations of the Jovian system from Voyager 1, *Science*, *204*, 972-976, 1979.

Hayward, T.L., J.W. Miles, J.R. Houck, G.E. Gull, and J. Schoenwald, SpectroCam-10: A 10-micron spectrograph/camera for the Hale telescope, *Proc. SPIE Int. Soc. Opt. Eng.*, *1946*, 334-340, 1993.

Henderson, B.G., and B.M. Jakosky, Near-surface thermal gradients and their effects on mid-infrared emission spectra of planetary surfaces, *J. Geophys. Res.*, *99*, 19,063-19,073, 1994.

Johnson, T.V., and C.B. Pilcher, Satellite spectrophotometry and surface compositions, in *Planetary Satellites*, edited by J.A. Burns, pp. 232-252, Univ. of Ariz. Press, Tucson, 1977.

Kahle, A.B., and A.F.H. Goetz, Mineralogic information from a new airborne thermal infrared multispectral scanner, *Science*, *222*, 24-27, 1983.

Lane, A.L., and D.L. Domingue, IUE's view of Callisto: Detection of an SO_2 absorption correlated to possible torus neutral wind alterations, *Geophys. Res. Lett.*, *24*, 1143-1146, 1997.

McCord, T.B., et al., Organics and other molecules in the surfaces of Callisto and Ganymede, *Science*, *278*, 271-275, 1997.

McCord, T.B., et al., Salts on Europa's surface detected by Galileo's Near Infrared Mapping Spectrometer, *Science*, *280*, 1242-1245, 1998.

McCord, T.B., et al., Hydrated salt minerals on Europa's surface from the Galileo Near Infrared Mapping Spectrometer (NIMS) investigation, *J. Geophys. Res.*, *104*, 11,827-11,851, 1999.

Moersch, J.E., and P.R. Christensen, Thermal emission from particulate surfaces: A comparison of scattering models with measured spectra, *J. Geophys. Res.*, *100*, 7465-7477, 1995.

Morrison, D., Radiometry of satellites and of the rings of Saturn, in *Planetary Satellites*, edited by J.A. Burns, pp. 269-291, Univ. of Ariz. Press, Tucson, 1977.

Nash, D.B., J.W. Salisbury, J.E. Conel, P.G. Lucey, and P.R. Christensen, Evaluation of infrared emission spectroscopy for mapping the Moon's surface composition from Lunar orbit, *J. Geophys. Res.*, *98*, 23,535-23,552, 1993.

Noll, K.S., R.E. Johnson, M.A. McGrath, and J.J. Caldwell, Detection of SO_2 on Callisto with the Hubble Space Telescope, *Geophys. Res. Lett.*, *24*, 1139-1142, 1997.

Rinsland, C.P., et al., ATMOS/ATLAS 3 infrared profile measurements of clouds in the tropical and subtropical upper troposphere, *J. Quant. Spectrosc. Radiat. Transfer*, *60*, 903-919, 1998.

Roush, T.L., J.B. Pollack, F.C. Witterborn, J.D. Bregman, and J.P. Simpson, Ice and minerals on Callisto: A reassessment of the reflectance spectra, *Icarus*, *86*, 355-382, 1990.

Salisbury, J.W., Mid-infrared spectroscopy: Laboratory data, in *Remote Geochemical Analysis: Elemental and Mineralogical Composition*, edited by C.M. Pieters and P.A.J. Englert, pp. 79-98, Cambridge Univ. Press, New York, 1993.

Salisbury, J.W., and D.M. D'Aria, Infrared (8 – 14 μm) remote sensing of soil particle size, *Remote Sens. Environ.*, *42*, 157-165, 1992.

Salisbury, J.W., and A. Wald, The role of volume scattering in reducing spectral contrast of Reststrahlen bands in spectra of powdered minerals, *Icarus*, *96*, 121-128, 1992.

Salisbury, J.W., D.M. D'Aria, and A. Wald, Measurements of thermal infrared spectral reflectance of frost, snow, and ice, *J. Geophys. Res.*, *99*, 24,235-24,240, 1994.

Salisbury, J.W., A. Basu, and E.M. Fischer, Thermal infrared spectra of lunar soils, *Icarus*, *130*, 125-139, 1997.

Spencer, J.R., The surfaces of Europa, Ganymede, and Callisto: An investigation using Voyager IRIS thermal infrared spectra, Ph.D. dissertation, Univ. of Ariz., Tucson, 1987a.

Spencer, J.R., Icy Galilean satellite reflectance spectra: Less ice on Ganymede and Callisto?, *Icarus*, *70*, 99-110, 1987b.

Spencer, J.R., Thermal segregation of water ice on the Galilean satellites, *Icarus*, *69*, 297-313, 1987c.

Spencer, J.R., L.K. Tamppari, T.Z. Martin, and L.D. Travis, Temperatures on Europa from Galileo photopolarimeter radiometer: Nighttime thermal anomalies, *Science*, *284*, 1514-1516, 1999.

Thomson, J.L., and J.W. Salisbury, The mid-infrared reflectance of mineral mixtures ($7 - 14$ μm), *Remote Sens. Environ.*, *45*, 1-13, 1993.

Urquhart, M.L., and B.M. Jakosky, Constraints on the solid-state greenhouse effect on the icy Galilean satellites, *J. Geophys. Res.*, *101*, 21,169-21,176, 1996.

Wald, A.E., Modeling thermal infrared ($2 - 14$ μm) reflectance spectra of frost and snow, *J. Geophys. Res.*, *99*, 24,241-24,250, 1994.

Warren, S.G., Optical constants of ice from the ultraviolet to the microwave, *Appl. Opt.*, *23*, 1206-1225, 1984.

M. E. Brown, Division of Geological and Planetary Sciences, MS 150-21, California Institute of Technology, Pasadena, CA 91125. (mbrown@gps.caltech.edu).

F. P. Mills, M/C 183-901, Jet Propulsion Laboratory, California Institute of Technology, 4800 Oak Grove Drive, Pasadena, CA 91109 (franklin.p.mills@jpl.nasa.gov).

(Received August 17, 1999; revised March 6, 2000; accepted March 8, 2000.)